TAB

Approved For Release 2000/08/08 : CIA-RDP96-00788R001500190001-6

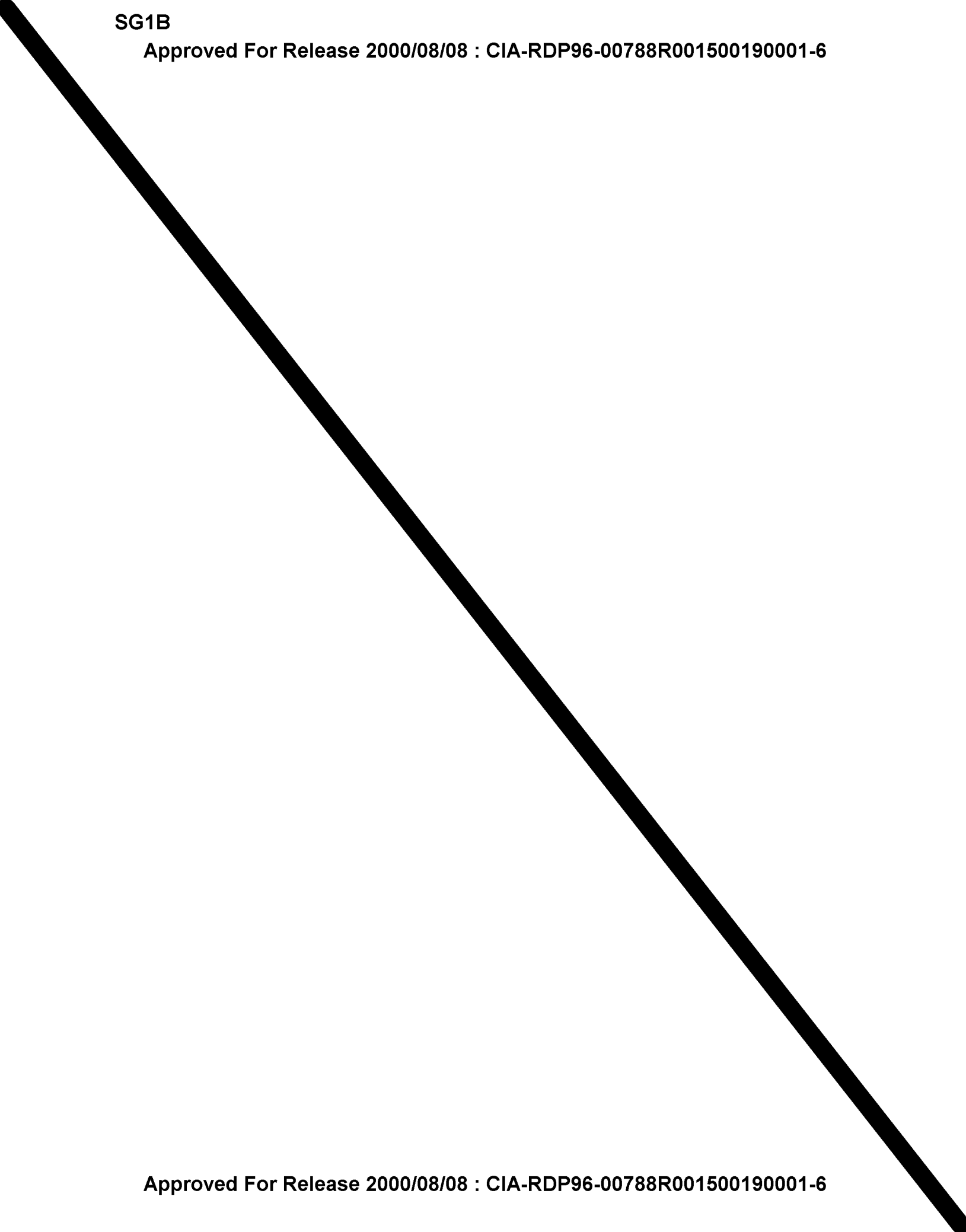

TAB

Approved For Release 2000/08/08 : CIA-RDP96-00788R001500190001-6

Next 1 Page(s) In Document Exempt

TAB

Approved For Release 2000/08/08 : CIA-RDP96-00788R001500190001-6

Next 4 Page(s) In Document Exempt

TAB

Approved For Release 2000/08/08 : CIA-RDP96-00788R001500190001-6

Next 5 Page(s) In Document Exempt

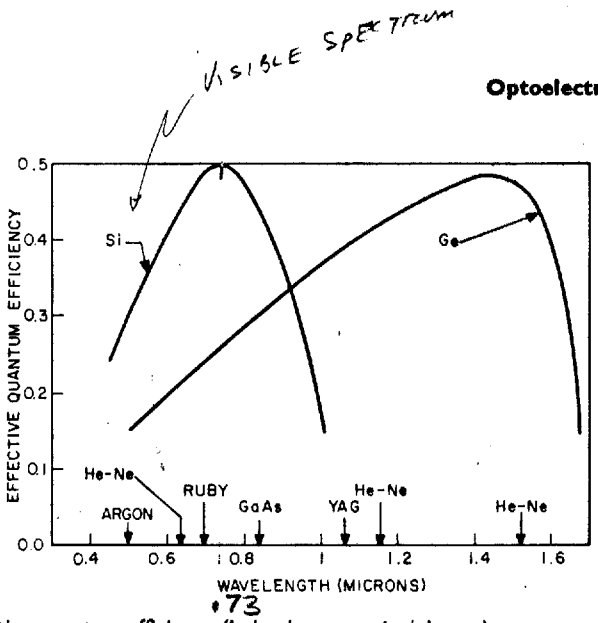

Fig. 24 Effective quantum efficiency (hole-electron pairs/photon) versus wavelength for Ge and Si photodetectors.
(After Melchior and Lynch, Ref. 39.)

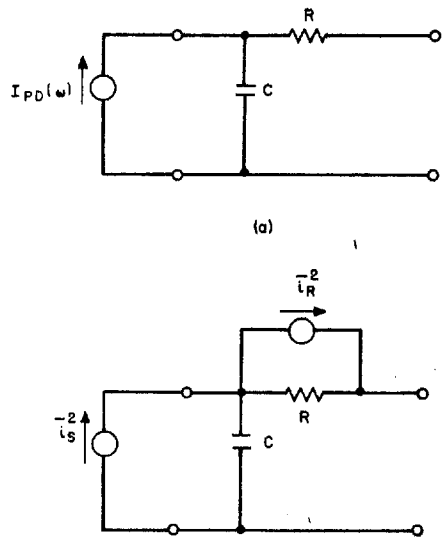

Fig. 25
(a) Equivalent circuit and
(b) noise equivalent circuit of a photodiode, where R is the series resistance and C is the junction capacitance.
(After DiDomenico and Svelto, Ref. 35.)

available power for the photo

$$P_{av} = \frac{1}{8}|I_{PD}(\omega)|$$

It is interesting to compare E For a typical photodiode with a photoconductor with the sar available power from the phot from the photoconductor.

The signal-to-noise perform equivalent noise circuit shown noise source due to the series source. The signal-to-noise ra

$$(S/N)_{power} = \frac{\eta}{4}$$

Comparing Eq. (44) with Eq. at high-level detection where SNR is comparable; at low-lev however, the SNR of the pho

B. The *p-i-n* Photodiode

depletion-layer photodetector. (the intrinsic layer) can be tai frequency response. A typical Fig. 26(a). Absorption of ligh pairs. Pairs produced in the de will eventually be separated by external circuit as carriers drif

Under steady-state conditio biased depletion layer is given

where J_{dr} is the drift current region and J_{diff} is the diffusion side the depletion layer in the b reverse-biased junction. We s assumptions that the thermal g surface n layer is much thinn electron generation rate is giv

SILICON CHARGED-PARTICLE DETECTORS

characteristics. The detector changes include increased noise and changes in voltage drop across the load resistor, which require adjustments to the applied bias voltage, which in turn change the electric-field strength. Thus carrier trapping and increased detector noise are degrading to energy resolution.

Resolution degradation appears as a broadening of the response for a monoenergetic source. With increasing doses of neutrons, charged particles, or fission fragments, the low-energy side of the response peak may begin to show a definite secondary peak. Continued irradiation results in further broadening, until, in extreme cases, the multiple peaks may merge completely. Electron bombardment tends to increase leakage current, resulting in excess detector noise, which broadens response peaks. Some of these damage effects may undergo a degree of annealing, but there is always a significant residual deterioration after a sufficient dose has been accumulated.

Partially depleted detectors are more susceptible than are fully depleted devices to deterioration from radiation damage. Radiation damage for different types of detectors are compared in Table 2, which gives the dose for various particles to significantly deteriorate the detectors.

OPERATING TEMPERATURE

As a rule of thumb, increasing the operating temperature of a charged-particle detector causes the leakage current to increase by a factor of 3 for each 10°C rise, resulting in a noise-width increase of approximately 1.7 keV per 10°C rise. The upper temperature limit is determined by the maximum acceptable noise or by the ultimate breakdown of the detector (usually between 45 and 55°C). *The effects of high-temperature breakdown are permanent* and are not covered by the warranty terms. An additional effect is the shift in detector bias caused by the higher leakage current. This leakage current increases the voltage drop across the series bias resistor, thus lowering the bias voltage across the detector. When high-temperature operation is necessary, a constant sensitive depth is maintained over the entire operating temperature range only if a totally depleted detector is used with sufficient overbias to compensate for the drop across the series bias resistor, which should be as small as possible (usually 1 to 3 MΩ is adequate).

Decreasing the operating temperature of the detector reduces junction noise and leakage current. However, the capacitance of the device is a constant limiting parameter of the system noise. Another limitation to successful operation at low temperatures is the expansion coefficient of the detector's component parts. The expansion coefficient is similar for silicon and for lavite, the ring in which the silicon wafer is mounted, but is quite different for the bonding epoxy. Therefore at very low temperatures the epoxy may crack, causing excessive noise or loss of contact. The probability of low-temperature damage increases with detector size. For cooled operation, detectors fabricated with cryogenic epoxy may be special ordered from ORTEC.

Another effect of decreasing the operating temperature of a silicon detector is an increase of the average energy necessary to create an electron-hole pair, ϵ. Due to a widening of the bandgap of silicon in the temperature range from 300 K to 80 K, ϵ increases from 3.62 eV to 3.72 eV. A result of this increase is an apparent shift in energy of a measured spectroscopic line. For instance, Fig. 8 shows the apparent peak shift of the 5.477-MeV ^{241}Am alpha particle peak in the 4.2-K to 320-K temperature range measured with silicon charged-particle detectors.

SHOCK AND VIBRATION

Many ORTEC surface-barrier detectors have been subjected to the shock and vibration tests required for

Table 2. Comparison of Radiation Damage in Silicon and Germanium Particle Detectors

Type of Detector	Radiation Damage (particles/cm^2)				
	Electrons	Fast Neutrons	Protons	Alpha Particles	Fission Fragments
Surface barrier	10^{13}	10^{12}	10^{10}	10^{9}	10^{8}
Diffusion junction	10^{13}	10^{12}	10^{10}	10^{9}	10^{8}
Si(Li)	10^{12}	10^{11}	10^{8}–10^{9}		
Ge(Li)		10^{8}–10^{9}			

#1

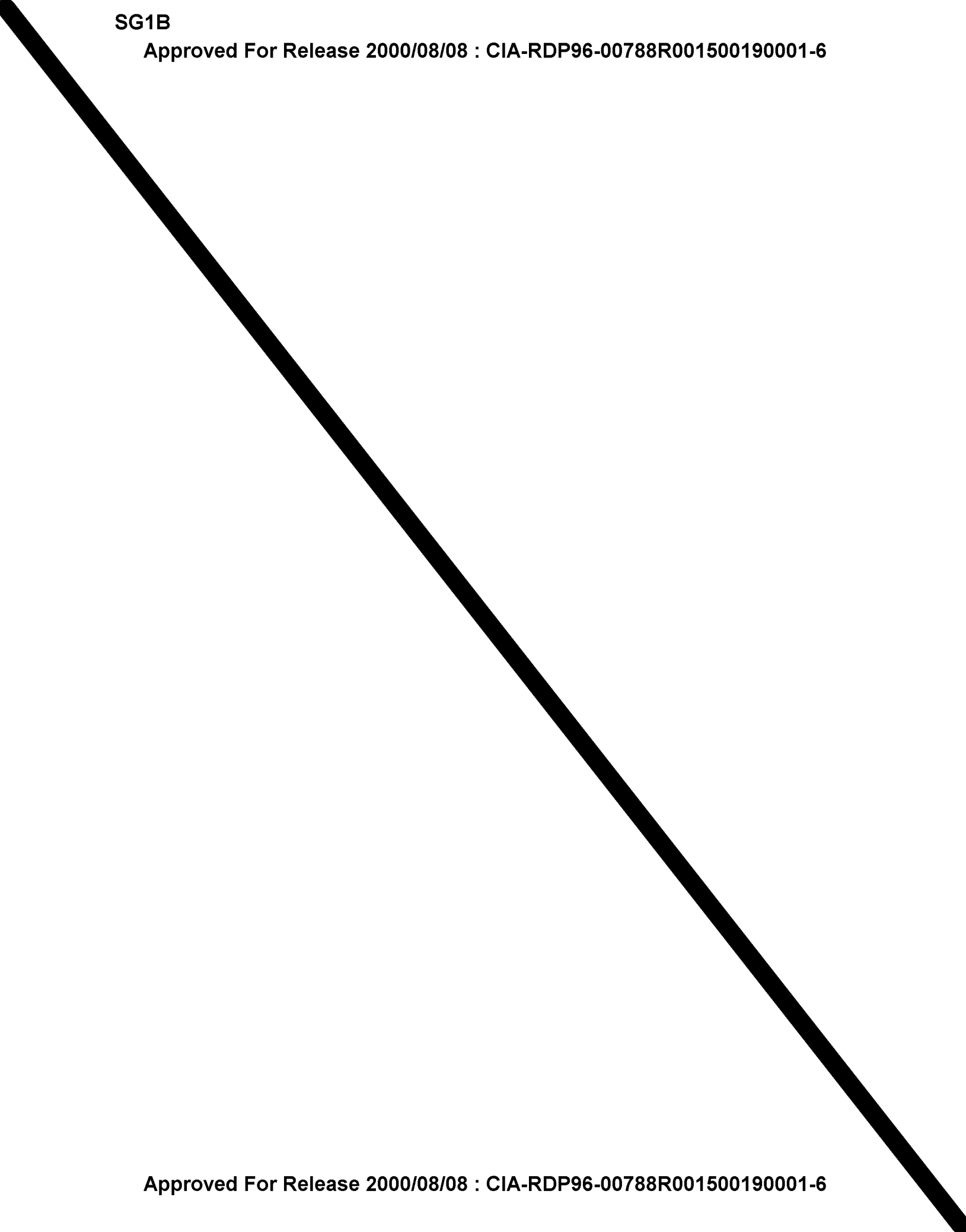

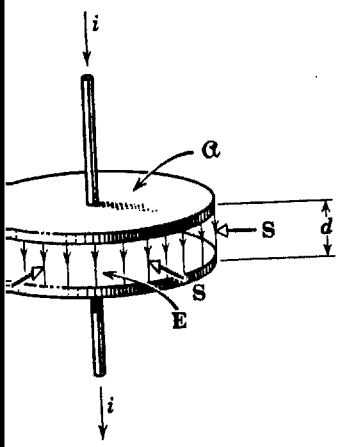

Fig. 39–17

inp arged. (*a*) Show that the
rli al volume. (*b*) Show that
ated by integrating the Poynting
s equal to the rate at which the

),

energy density for all points within
he Poynting vector point of view,
gh the wires but through the space
we must first find **B**, which is the
ing the charging process; see Fig.

Nature and Propagation of Light

CHAPTER 40

40–1 Light and the Electromagnetic Spectrum

Light was shown by Maxwell to be a component of the *electromagnetic spectrum* of Fig. 40–1. All these waves are electromagnetic in nature and have the same speed c in free space. They differ in wavelength (and thus in frequency) only, which means that the sources that give rise to them and the instruments used to make measurements with them are rather different.* The electromagnetic spectrum has no definite upper or lower limit. The labeled regions in Fig. 40–1 represent frequency intervals within which a common body of experimental technique, such as common sources and common detectors, exists. All such regions overlap. For example, we can produce radiation of wavelength 10^{-3} meter either by microwave techniques (microwave oscillators) or by infrared techniques (incandescent sources).

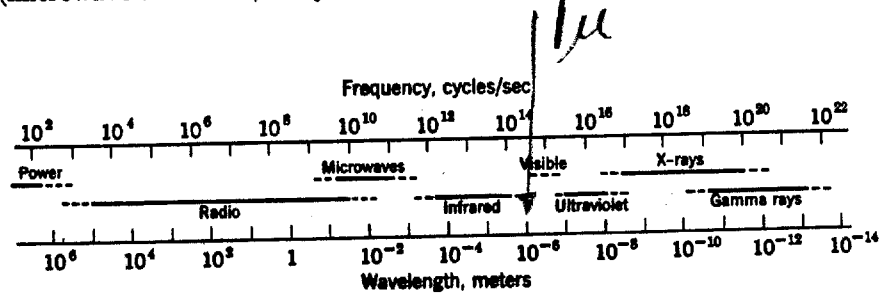

Fig. 40–1 The electromagnetic spectrum. Note that the wavelength and frequency scales are logarithmic.

* For a report of electromagnetic waves with wavelengths as long as 1.9×10^7 miles the student should consult an article by James Heirtzler in the *Scientific American* for March 1962.

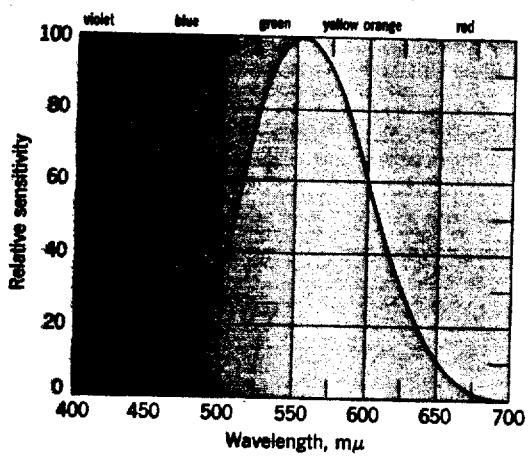

Fig. 40–2 The relative eye sensitivity of an assumed *standard observer* at different wavelengths for normal levels of illumination. The shaded areas represent the (continuously graded) color sensations for normal vision.

"Light" is defined here as radiation that can affect the eye. Figure 40–2, which shows the relative eye sensitivity of an assumed *standard observer* to radiations of various wavelengths, shows that the center of the visible region is about 5.55×10^{-7} meter. Light of this wavelength produces the sensation of yellow-green.*

In optics we often use the micron (abbr. μ) the millimicron (abbr. mμ), and the Angstrom (abbr. A) as units of wavelength. They are defined from

$$1\ \mu = 10^{-6}\ \text{meter}$$

$$1\ \text{m}\mu = 10^{-9}\ \text{meter}$$

$$1\ \text{A} = 10^{-10}\ \text{meter}.$$

Thus the center of the visible region can be expressed as 0.555 μ, 555 mμ, or 5550 A.

The limits of the visible spectrum are not well defined because the eye sensitivity curve approaches the axis asymptotically at both long and short wavelengths. If the limits are taken, arbitrarily, as the wavelengths at which the eye sensitivity has dropped to 1% of its maximum value, these limits are about 4300 A and 6900 A, less than a factor of two in wavelength. The eye can detect radiation beyond these limits if it is intense enough. In many experiments in physics one can use photographic plates or light-sensitive electronic detectors in place of the human eye.

* See "Experiments in Color Vision" by Edwin H. Land, *Scientific American*, May 1959, and especially "Color and Perception: the Work of Edwin Land in the Light of Current Concepts" by M. H. Wilson and R. W. Brocklebank, *Contemporary Physics*, December 1961, for a fascinating discussion of the problems of perception and the distinction between color as a characteristic of light and color as a perceived property of objects.